

MODELLING TEXTURE DEVELOPMENT OF ZIRCONIUM ALLOYS AT HIGH TEMPERATURES

R.A. Lebensohn¹, P.V. Sanchez² and A.A. Pochettino²

(1) Instituto de Física Rosario (CONICET-UNR)

Bv. 27 de Febrero 210 bis, 2000 Rosario, Argentina.

(2) Dpto. Ciencias de Materiales, Gcia. Desarrollo, CNEA,
Avda. Libertador 8250, 1429 Buenos Aires, Argentina.

(Received June 6, 1993)
(Revised November 12, 1993)

Introduction

Temperature has a great influence on the relative critical resolved stresses (CRSS) of the potentially active deformation modes of zirconium and zirconium alloys. Therefore, rather different deformation textures are obtained at different temperatures. It is well known that $\{1100\}\langle 1120 \rangle$ slip (or prismatic $\langle a \rangle$) is the most active mode in a wide range of temperatures [1-2]. Nevertheless, since prismatic slip does not suffice for accommodating an arbitrary imposed strain, other deformation modes must be activated. It is well established [1-3-4] that $\{1012\}\langle 1011 \rangle$ 'tensile' twinning and also $\{1011\}\langle 1123 \rangle$ 'compressive' twinning are mostly active at low and intermediate temperatures. On the other hand, at high temperatures, further twinning activity is prevented and non-prismatic slip modes become active. Pyramidal $\langle c+a \rangle$ ($\{1011\}\langle 1123 \rangle$), pyramidal $\langle a \rangle$ and ($\{1101\}\langle 1120 \rangle$) and basal $\langle a \rangle$ ($\{0001\}\langle 1120 \rangle$) are the possible modes that can complement the deformation pattern. Pyramidal $\langle c+a \rangle$ activity has been reported by many authors [5-6]. Among them, Pochettino et al [7] have analyzed the contribution of $\langle c+a \rangle$ pyramidal slip on plastic deformation of polycrystalline hcp materials. They have shown that, even at room temperature, an important activity of $\langle c+a \rangle$ slip can be observed in grains presenting an adequate orientation. From transmission electron microscopy observations, they also point out that reactions between $\langle c+a \rangle$ and $\langle a \rangle$ dislocations may sometimes produce pyramidal $\langle a \rangle$ slip. Basal $\langle a \rangle$ has been reported by Akhtar [2], but there are not many experimental evidences about its activity in polycrystals.

The aim of this paper is to determine the best combination of slip modes and CRSS for the calculation of texture development in hot-rolled zirconium alloys. Texture predictions were performed using two different approaches to the macro-microstructural correlation: the classical Taylor model and the self consistent formulation. Predicted (0002) pole figures are compared with experimental results, which have been obtained for different Zr alloys and rolling conditions.

Details of the Calculation

Any scheme for the calculation of texture development must be based on a reliable hypothesis about the way in which the polycrystal strain rate and stress $-\dot{\epsilon}$ and Σ , respectively- and the corresponding magnitudes of the constituent grains $-\epsilon$ and σ - are correlated. Two models are used in this work: the classical Taylor (or full constraints: FC) model, that assumes equal strain in every grain and the self-consistent formulation (SC) that allows each grain

to deform differently, according to its directional properties and depending on the strength of the interaction between the grain and its surroundings (for details see [4]). In both cases, a viscoplastic constitutive equation is assumed for the single crystal:

$$\dot{\epsilon} = \gamma_0 \sum_s m^s \left(\frac{m^s \sigma}{\tau_c^s} \right)^n \quad (1)$$

where s identifies the active deformation systems, m^s is the Schmid tensor, τ_c^s is the CRSS of each system, n is the inverse of the rate-sensitivity coefficient and γ_0 is a scaling factor. If E is imposed to the polycrystal, FC hypothesis can be expressed as:

$$\dot{\epsilon} = \gamma_0 \sum_s m^s \left(\frac{m^s \sigma}{\tau_c^s} \right)^n = \dot{E} \quad (2)$$

Once the value of σ for each grain is obtained, the macroscopic stress can be calculated as:

$$\Sigma = \langle \sigma \rangle \quad (3)$$

where the symbol $\langle \rangle$ denotes a weighted average over the constituent grains. On the other hand SC formulation is based on the interaction equation that relates the deviation of microscopic strain rate and stress from the corresponding macroscopic magnitudes:

$$\dot{\epsilon} - \dot{E} = -\tilde{M}(\sigma - \Sigma) \quad (4)$$

The interaction tensor \tilde{M} can be calculated from the expression:

$$\tilde{M} = n(I - S)^{-1} S M \quad (5)$$

where S is the viscoplastic Eshelby tensor, M is the macroscopic secant compliance modulus that relates E and Σ through the expression $E = M \Sigma$ and n is the same as in equation (1). Since Σ , and so M , are not known a priori, an initial guess must be made for M and its value must be adjusted self-consistently.

Results

Figure 1 shows different experimental (0002) pole figures for zirconium alloys rolled at high temperature. Although these pole figures correspond to materials having different alloy content and different deformation history, all of them are characterized by a high concentration of basal poles around ND. These experimental results are included here in order to compare them with calculated pole figures corresponding to texture simulations carried out using different sets of slip modes. To start with, all the combinations include prismatic slip as an active mode, with the lowest CRSS (fixed as $\tau_{pr}=1$). In case 1, prismatic slip is combined with pyramidal $\langle c+a \rangle$ slip ($\tau_{py\langle c+a \rangle}=3$). In cases 2 and 3 pyramidal $\langle a \rangle$ and basal slip are also considered. These three cases show the effect of including a relatively 'soft' pyramidal $\langle c+a \rangle$ slip. Nevertheless, the experimental evidence indicates that $\tau_{py\langle c+a \rangle}$ is around 10 times higher than prismatic slip. Therefore, case 4 is selected from Akhtar [5] for $T=970^\circ\text{K}$. Both FC and SC calculations, starting from a random texture, for a value of $n=7$ and a final true strain $\epsilon=1$ (63% thickness reduction) are reported here. Table 1 shows the relative activity of the different slip modes for the initial and final stages of deformation.

Case 1: $\tau_{pr}=1$, $\tau_{py\langle c+a \rangle}=3$ (figs. 2a-2b). The RD maximum in FC texture is typically associated to a high pyramidal $\langle c+a \rangle$ activity (see Table I). In SC case, TD maximum can be attributed to the self-consistent rotations [4] associated with high activity of prismatic slip.

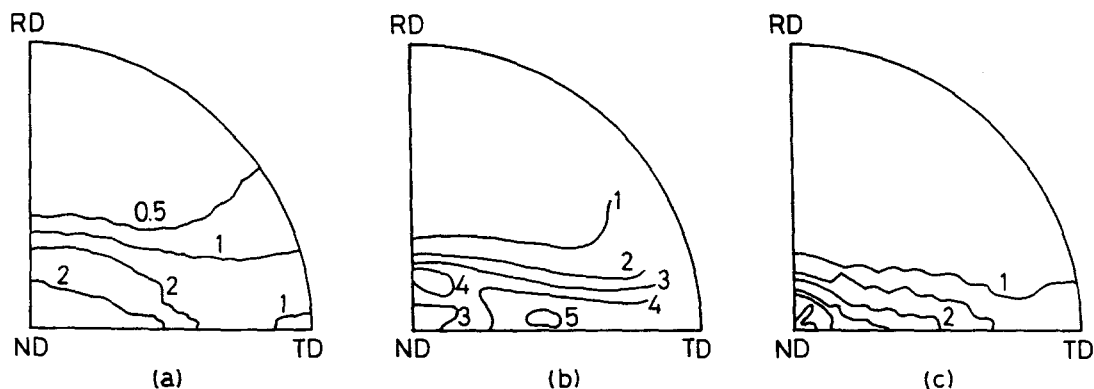


Fig. 1. Experimental (0002) pole figures: (a) Zr-2,5%Nb hot rolled at 970°K [8], (b) Zircaloy-2 hot rolled at 1173°K and then rolled at 623°K [9], (c) Zircalloy-4 rolled at 870°K.

TABLE I

CASE	MODEL	ϵ	A C T I V I T Y			
			pr	py<a>	bas<a>	py<c+a>
- 1 - $\tau_{pr}=1$ $\tau_{py<c+a>}=3$	FC	$\epsilon=2.5\%$	25%	--	--	75%
		$\epsilon=100\%$	27%	--	--	73%
	SC	$\epsilon=2.5\%$	68%	--	--	32%
		$\epsilon=100\%$	61%	--	--	39%
- 2 - $\tau_{pr}=1$ $\tau_{py<a>}=1.5$ $\tau_{py<c+a>}=3$	FC	$\epsilon=2.5\%$	11%	57%	--	33%
		$\epsilon=100\%$	11%	53%	--	36%
	SC	$\epsilon=2.5\%$	38%	45%	--	17%
		$\epsilon=100\%$	37%	42%	--	21%
- 3 - $\tau_{pr}=1$ $\tau_{b<a>}=1.5$ $\tau_{py<c+a>}=3$	FC	$\epsilon=2.5\%$	34%	--	31%	35%
		$\epsilon=100\%$	32%	--	28%	40%
	SC	$\epsilon=2.5\%$	54%	--	39%	7%
		$\epsilon=100\%$	50%	--	36%	14%
- 4 - $\tau_{pr}=1$ $\tau_{b<a>}=1.5$ $\tau_{py<c+a>}=10$	FC	$\epsilon=2.5\%$	36%	--	34%	31%
		$\epsilon=100\%$	35%	--	26%	39%
	SC	$\epsilon=2.5\%$	58%	--	42%	0.0%
		$\epsilon=100\%$	57%	--	43%	0.1%

Case 2: $\tau_{pr}=1$, $\tau_{py<a>}=1.5$, $\tau_{py<c+a>}=3$ (figs. 2c-2d). The selection of these sets of CRSS is made on the basis of a recent study [3] of the main topological domains of the single crystal yield surface of hexagonal materials. It was determined that the inclusion of pyramidal <a> mode changes significantly the final texture only if $\{\tau_{py<c+a>}/\tau_{py<a>}\} > 1.25$. In the FC texture two stable

components appear: a RD maximum associated with pyramidal $\langle c+a \rangle$ slip and a partial fiber with a maximum tilted about 35° from ND, due to a high pyramidal $\langle a \rangle$ activity. A similar result is obtained under the SC scheme, except for a weaker RD component due to a lowering in pyramidal $\langle c+a \rangle$ activity.

Case 3: $r_{pr}=1$, $r_{b\langle a \rangle}=1.5$, $r_{py\langle c+a \rangle}=3$ (figs. 2e-2f). The replacement of pyramidal $\langle a \rangle$ by another slip mode having the same $\langle a \rangle$ -Burgers vector (vg. basal slip) does not lead to a significantly different FC texture. In the SC case, a higher prismatic and basal activity leads to a concentration of the texture around ND, together with a weakening of RD component and the appearance of a maximum in TD. This case reveals that a high concentration of basal poles around ND can be associated to a high activity of prismatic and basal slip at the expense of pyramidal $\langle c+a \rangle$ slip.

Case 4: $r_{pr}=1$, $r_{b\langle a \rangle}=1.5$, $r_{py\langle c+a \rangle}=10$ (figs. 2g-2h). This case is selected from Akhtar [5] for $T=970^\circ\text{K}$. In the FC case, although a weak RD component remains in place, an important ND concentration, with a maximum tilted 20° towards RD is obtained. In the SC case, the RD maximum disappears, the TD intensity is slightly reinforced and two maxima are formed near ND, tilted 20° towards RD and TD, respectively.

Discussion and Conclusions

It is evident from case 4 that the use of a 'hard' pyramidal $\langle c+a \rangle$ mode leads to simulated textures that are in good agreement with the experimental evidence. This agreement reveals a coherence between measured values of CRSS, experimental textures and theoretical predictions.

Another interesting conclusion can be obtained from the comparison between FC and SC results. While at low temperature FC and SC formulations drive to substantially different textures [4], no great differences can be found between FC and SC textures at high temperature, meaning that the polycrystal becomes less plastically anisotropic. A lower value of the exponent n (eq.2), meaning that the material becomes more viscous when the temperature rises, together with the replacement of twinning systems by slip systems are responsible for the changes in polycrystal plastic behavior.

In order to complete the analysis of texture evolution during hot rolling processes two aspects of the problem must be pointed out:

1) *The effect of the initial texture:* Generally, before hot rolling, the material was transformed by forging or by extrusion, producing an "initial texture" for the rolling process which could alter the final texture. This possible effect is analyzed for the case of hot rolling, where it does not seem to be outstanding. Figs. 3a-3b show schematically the evolution of $\langle c \rangle$ axes when FC and SC formulations are used in texture predictions. In these figures, numbers 3 and 4 are associated to the limit of the reorientation domains for the set of CRSS values corresponding to the cases 3 and 4 respectively. Initially, the material was assumed to be isotropic. Comparing these evolutions with experimental and predicted (0002) pole figures, we conclude that:

- Texture formation in the ND/TD region is essentially related to the choice of the model (FC or SC) used to describe texture evolution. In the case of the SC formulation, the only effect of the initial texture is that $\langle c \rangle$ axes placed near the RD-TD circle contribute to increase the pole density around the TD.

- The effect of the initial texture on the final (0002) pole density around RD seems to be important for FC formulation and "soft" pyramidal $\langle c+a \rangle$ slip. It is not easy to conclude if the low pole density predicted around RD, which agrees with experiments in the case 4, is a consequence of the choice of an adequate and more realistic formulation (SC) together with a correct set of CRSS, or it is associated to an initial texture presenting a low $\langle c \rangle$ density around the RD.

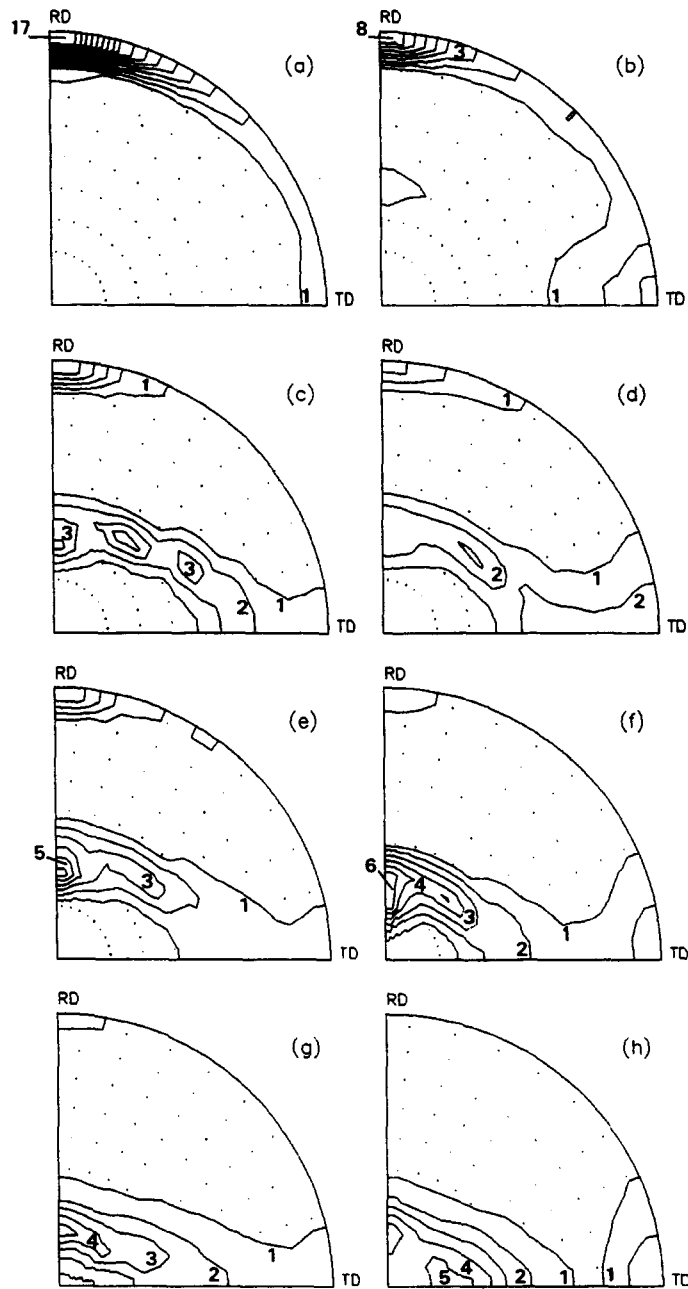


FIG 2. Predicted (0002) pole figures using FC and SC formulations and different CRSS values: (a-b) $\tau_{pr}=1$, $\tau_{py\langle c+a \rangle}=3$; (c-d) $\tau_{pr}=1$, $\tau_{py\langle a \rangle}=1.5$, $\tau_{py\langle c+a \rangle}=3$; (e-f) $\tau_{pr}=1$, $\tau_{b\langle a \rangle}=1,5$, $\tau_{py\langle c+a \rangle}=3$; (g-h) $\tau_{pr}=1$, $\tau_{b\langle a \rangle}=1,5$, $\tau_{py\langle c+a \rangle}=10$.

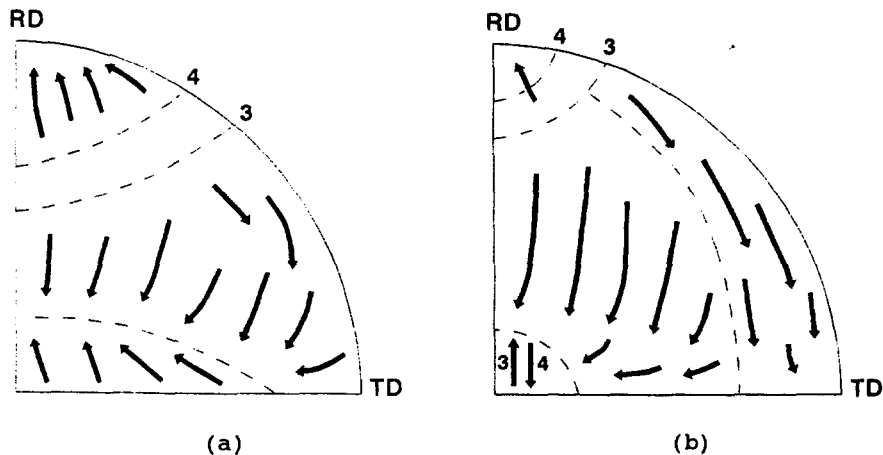


FIG 3. $\langle c \rangle$ axes evolutions in hot rolled Zr for CRSS corresponding to cases 3 and 4: (a) FC, (b) SC formulation.

2) *Static recrystallization effects introduced after rolling:* In the case of cold rolled Zr alloys, it was observed that static recrystallization introduces a small reorientation of c -axes ($5-10^\circ$) towards ND and a rotation of $\langle a \rangle$ axes of 30° around the c -axis of crystals [10]. Then, if some recrystallization occurs after rolling, its effect can contribute to concentrate $\langle c \rangle$ axes near the ND direction and, in another way, to diminish the effective reorientation introduced by basal slip activity, which seems to be too high in our calculations. This additional reorientation of $\langle c \rangle$ axes towards ND could be accounted by setting a higher $(\tau_{py}\langle c+a \rangle / \tau_b\langle a \rangle)$ relationship.

In conclusion, an adequate choice of the formulation for the description of the mechanical behavior of the material together with reliable CRSS values allow to obtain an acceptable description of hot rolling texture evolution in Zr alloys. Nevertheless, attention must be paid to metallurgical aspects related to initial textures introduced by previous thermo-mechanical treatments and possible recrystallization after rolling.

Acknowledgements

This work was partially supported by the Proyecto Multinacional de Investigación y Desarrollo (OEA-CNEA). Authors would also like to thank Dr. Brigitte Bacroix for the determination of pole figure presented in Fig.1.c.

References

1. E. Tenckoff, Metall. Trans. A, **9A**, 1401, (1978).
2. A. Akhtar, Acta Metallurgica, **21**, 1 (1973).
3. C. Tomé, R. Lebensohn, U.F. Kocks, Acta Metall. **39**, 2667 (1991).
4. R. Lebensohn, C. Tomé, Acta Metall., in press.
5. A. Akhtar, J. Nuclear Mat. **47**, 79, (1983).
6. E. Tenckoff, Z. Metallk., **63**, 4, (1972).
7. A.A. Pochettino, N. Gannio, C. Vial Edwards, R. Penelle, Scripta Metall., **27**, 1859, (1992).
8. A. Salinas, Ph.D. Thesis, Mc Gill University, (1988).
9. R.G. Ballinger, The Anisotropic Mechanical Behaviour of Zircaloy-2, p.45, Garland Publishing Inc., N. York & London, (1979).
10. M.I. González, private communication, (1992).